IUST Iran University of Science and Technology

Iranian Journal of Electrical and Electronic Engineering

Journal Homepage: ijeee.iust.ac.ir

Research Paper

Modelling of High Quantum Efficiency Avalanche Photodiode

T. Baldawi* and A. Abuelhaija**(C.A.)

Abstract: A model of a low noise high quantum efficiency n^+np Germanium Photodiode utilizing ion implantation technique and subsequent drive-in diffusion in the n layer is presented. Numerical analysis is used to study the influence of junction depth and bulk concentration on the electric field profile and quantum efficiency. The performance of the device is theoretically treated especially at the wave-length region 1.55μm where the Silica optical fiber has minimum attenuation loss. It has been found that at this wave-length and for the optimum device design the quantum efficiency approaches about 90%.

Keywords: Avalanche Photodiodes, Responsivity, Quantum Efficiency.

1 Introduction

THE quantum efficiency of the avalanche photodiode has been treated in this work. Quantum Efficiency (QE) could be defined as the number of electrons collected to the number of the incident photons. Let us define first the Responsivity R of a photo-detector which can be expressed mathematically as given in literature [1-4] as:

$$R = \frac{\text{Photo Current}\left(I_{ph}\right)}{\text{Incident Optical Power}\left(P_o\right)} = \left(\frac{q}{h\nu}\right)\left(1-r\right)\left(1-e^{-\alpha x}\right) \quad (1)$$

where q is the electronic charge, $(P_o/h\nu)$ is the number of incident photons per second, r is the reflectivity at air to semiconductor interface, and $(1–e^{-\alpha x})$ is the fraction absorbed in the semiconductor.

The responsivity could be re-written as:

$$R = \eta_e\left(\frac{q}{h\nu}\right) = \eta_e\left(\frac{\lambda}{1.24}\right) \quad (2)$$

where λ is the wavelength and η_e is the external quantum efficiency defined as:

$$\eta_e = \frac{\text{No. of Electrons Collected}}{\text{No. of Incident Photons}} = \frac{\left(\frac{I_{ph}}{q}\right)}{\frac{P_o}{h\nu}} \quad (3)$$

or

$$\eta_e = \left(1-r\right)\left(1-e^{-\alpha x}\right) \quad (4)$$

and the internal quantum efficiency is defined as:

$$\eta_i = \frac{\eta_e}{1-r} = \left(1-e^{-\alpha x}\right) \quad (5)$$

where α is the optical absorption coefficient given as $\alpha \approx 10^2–10^3$ cm^{-1} for Si (Indirect–bandgap), and $\alpha \approx 10^4$ cm^{-1} for Si (direct–bandgap).

2 Analysis and Modelling

The device structure is shown in Fig. 1. The n^+ layer of thickness 0.3 μm is formed by arsenic diffusion, so most of the light is absorbed in the n layer. This thin n^+ layer reduces the holes that has been lost by surface and bulk recombination during transportation toward the junction when the light is absorbed in this layer. The n layer is formed by Arsenic ion implantation and subsequent drive-in diffusion. The p layer is a Gallium doped substrate.

The n layer is the key layer of this device with a Gaussian distribution given by:

$$C\left(x\right) = \frac{Q_o}{\sqrt{\pi Dt}} e^{\left(\frac{-x^2}{4Dt}\right)} \quad (6)$$

Iranian Journal of Electrical and Electronic Engineering, 2019.
Paper first received 12 June 2018, revised 19 March 2019, and accepted 20 March 2019.
* The author is with the Department of Electrical Engineering, Princess Sumaya University for Technology, Amman, Jordan.
E-mail: t.albaldawi@psut.edu.jo.
** The author is with the Electrical Engineering Department, Applied Science Private University, Amman, Jordan.
E-mail: a_abualhijaa@asu.edu.jo.
Corresponding Author: A. Abuelhaija.

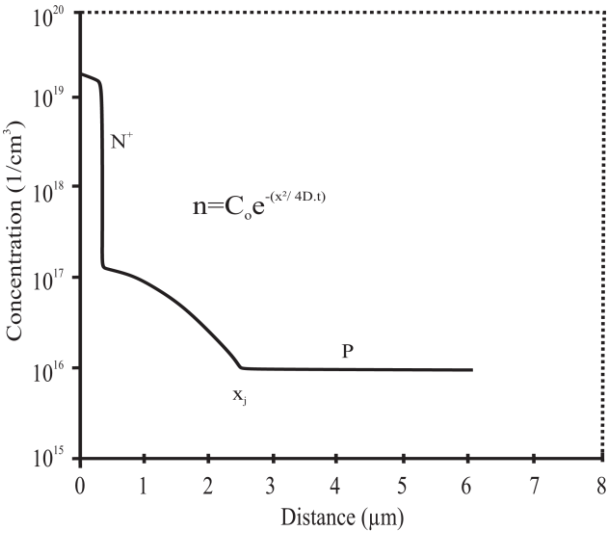

Fig. 1 Doping profile of n^+-*n*-*p* germanium avalanche photodiode.

where C is the impurity density at a distance X from the surface, Q_o is the implantation dose, D is the diffusion coefficient of Arsenic, and t is the diffusion time.

The Gaussian distribution can be written as:

$$C(x) = C_o e^{\left(\frac{-x^2}{4Dt}\right)} \tag{7}$$

where $C_o = Q_o / \sqrt{\pi D \cdot t}$ is the surface concentration.

The junction depth may be defined as:

$$C_o e^{\left(\frac{-x_j^2}{4Dt}\right)} = C_B \tag{8}$$

where C_B is the background doping level, and x_j is the junction depth.

It can be seen from the doping profile that the net impurity density varies gradually as in the case of linearly graded junction at one side of the junction, whereas deep into the semiconductor the doping level is as in the case of abrupt junction. So the diffused junction must be treated as a middle case between abrupt and linearly graded junction. The complete modelling process employed in this work is shown in Fig. 2, here the modelling of the electric field, quantum efficiency and the *I-V* characteristics will be treated only.

2.1 Electric Field Distribution

Doping profile and electric field distribution is illustrated in Fig. 3, where a_1 and a_2 are the two components of the depletion layer thickness. The net density of positive charge ρ, lying within the depletion layer can be written as:

$$\rho = q(C - C_B) \tag{9}$$

The Poisson's equation can be written as:

$$\frac{d^2\phi}{dx^2} = \frac{-qC_o}{\varepsilon_o \varepsilon_r}\left[e^{\left(\frac{-x_j^2}{4Dt}\right)} - \frac{C_B}{C_o}\right] \tag{10}$$

where ϕ is the electrostatic potential, ε_r is the dielectric constant of the material, and ε_o is the permittivity of free space.

Fig. 3 indicates that the electric field vanishes at the depletion layer boundaries. Thus by integrating Poisson's equation, an expression for the field distribution on the two sides of the junction is found. On the left side the field is $E_1(x)$, where:

$$E_1(x) = \frac{qC_o}{\varepsilon_o \varepsilon_r}\sqrt{\pi Dt}\left[erf\left(\frac{x}{\sqrt{4D \cdot t}}\right) - erf\left(\frac{x_j - a_1}{\sqrt{4Dt}}\right)\right] - \left(\frac{C_B}{C_o}\right)\left(x - x_j + a_1\right) \tag{11}$$

and on the right side, the electric field $E_2(x)$ is given by:

$$E_2(x) = \frac{qC_o}{\varepsilon_o \varepsilon_r}\sqrt{\pi Dt}\left[erf\left(\frac{x}{\sqrt{4Dt}}\right) - erf\left(\frac{x_j - a_2}{\sqrt{4Dt}}\right)\right] - \left(\frac{C_B}{C_o}\right)\left(x - x_j + a_2\right) \tag{12}$$

The expression for peak field are found immediately by substituting x_j for x in (11) and (12), giving:

$$E_1(x_j) = \frac{qC_o}{\varepsilon_o \varepsilon_r}\left[\sqrt{\pi Dt}\left(erf\left(\frac{x_j}{\sqrt{4Dt}}\right) - erf\left(\frac{x_j - a_1}{\sqrt{4Dt}}\right)\right) - a_1 e^{\frac{-x_j^2}{4Dt}}\right] \tag{13}$$

$$E_2(x_j) = \frac{qC_o}{\varepsilon_o \varepsilon_r}\left[\sqrt{\pi Dt}\left(erf\left(\frac{x_j}{\sqrt{4Dt}}\right) - erf\left(\frac{x_j - a_2}{\sqrt{4Dt}}\right)\right) - a_2 e^{\frac{-x_j^2}{4Dt}}\right] \tag{14}$$

Since the field is continuous at the junction, so the relation between a_1 and a_2 can be obtained, that is

$$E_1\left(x_j, \frac{C_B}{C_o}, a_1\right) = E_2\left(x_j, \frac{C_B}{C_o}, a_2\right) \tag{15}$$

This equation is solved by Newton Raphson method using the trancedental equations [5, 6]. The electric field $E(x)$ for various values of junction depth and bulk concentration is shown in Figs. 4 and 5.

2.2 Quantum Efficiency

The quantum efficiency can be modelled in the n^+np structure by assuming three currents density equations [7-9], one at the junction between the n^+ and the n layer , the other current density is at the depletion region and the third one is from the p layer as shown in Fig. 6.

The expression of the continuity equation in the n^+

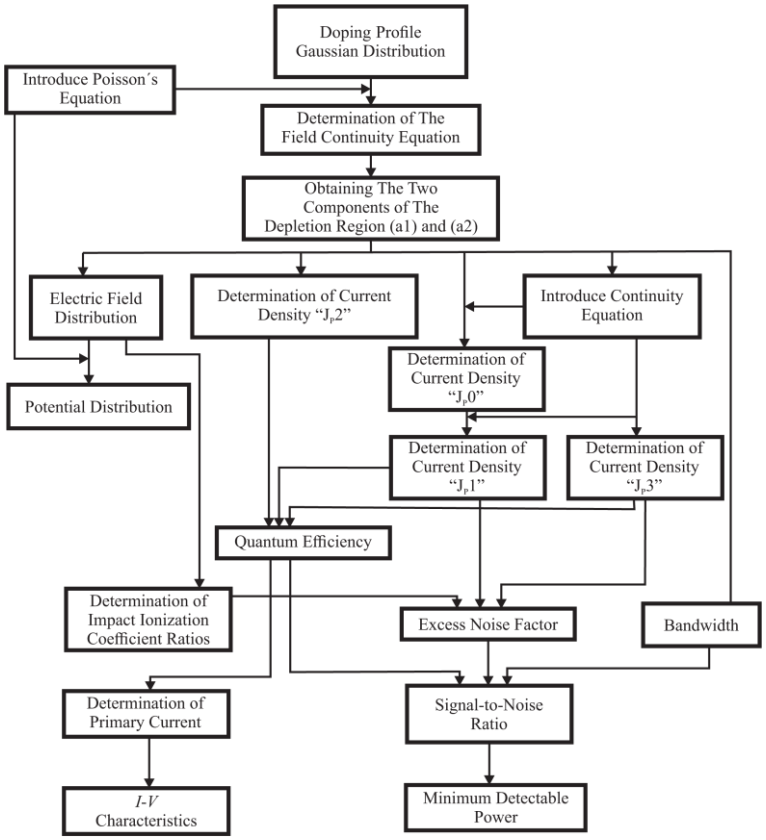

Fig. 2 Block diagram of the modelling process employed in the analysis of the n^+-n-p germanium avalanche photodiode.

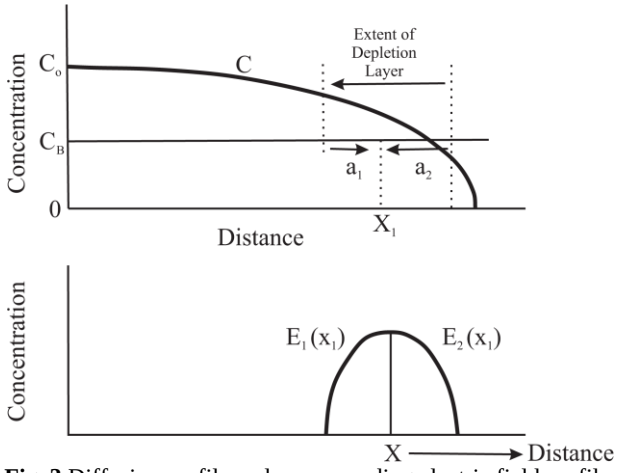

Fig. 3 Diffusion profile and corresponding electric field profile.

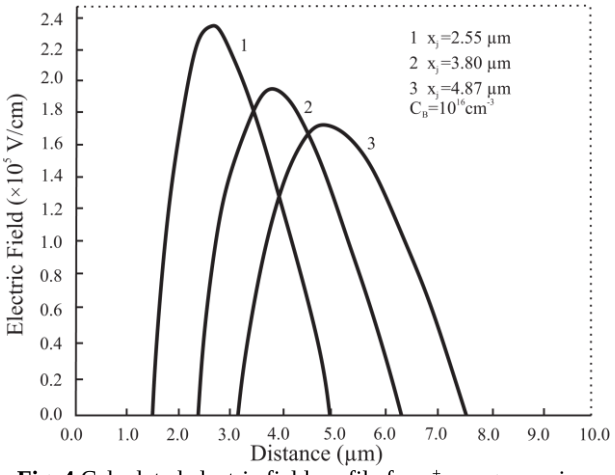

Fig. 4 Calculated electric field profile for n^+-n-p germanium avalanche photodiode for different junction depths at a multiplication factor of 10.

layer is given by:

$$D_P \frac{d^2 P_{n^+}}{dx^2} + \alpha F e^{-\alpha x} - \frac{P_{n^+} - P_{n^+}(0)}{\tau_P} = 0 \qquad (16)$$

where P_{n+} is the hole density in the n+ layer, $P_{n+}(0)$ is the hole density at thermal equilibrium, D_P is the diffusion constant, α is the absorption coefficient, F is the number of incident photons per square centimeter per second, and τ_P is the minority carrier life time.

The boundary conditions are:

1. At the surface, we have surface recombination with recombination velocity (S_P):

$$D_P \frac{d\left(P_{n^+} - P_{n^+}(0)\right)}{dx} = S_P \left[P_{n^+} - P_{n^+}(0)\right], \text{atx=0} \qquad (17)$$

2. At the depletion edge, the excess carrier density is small due to the electric field in the depletion region:

$$P_{n^+} - P_{n^+}(0) = 0, \text{atx=W} \qquad (18)$$

where W is the width of the n^+ layer.

The resulting photo-current density according to the above boundary conditions is given by:

$$J_{P0}=\frac{qF\alpha L_P}{\alpha^2L^2-1}\left[\left(\frac{S_PL_P}{D_P}\right)-exp\left(-\alpha W\right)\left(\frac{S_PL_P}{D_P}cosh\left(\frac{W}{L_P}\right)+sinh\left(\frac{W}{L_P}\right)\right)-\alpha L_P exp\left(-\alpha W\right)\right] \quad (19)$$

where $L_P=\sqrt{D_P\tau_P}$ is the diffusion length of holes.

The photo-current density (J_{P1}) injected into the depletion layer at $X = X_1–a_1$ can be derived from the following conditions:

Condition (a):

$$qD_{P1}\frac{d\left(P-P_n\left(0\right)\right)}{dx}=J_{P0}, \text{atx=W} \quad (20)$$

where D_{P1} is the diffusion constant of holes in the n layer, P_n is the hole concentration, and $P_n(0)$ is the hole concentration at thermal equilibrium.

Condition (b):

$$P-P_n\left(0\right)=0, \text{ at } x=x_j-a_1 \quad (21)$$

So,

$$J_{P1}=\frac{J_{P0}}{cosh\left(\frac{x_j-a_1-W}{L_{P1}}\right)}-\frac{qF\alpha^2L_{P1}^2}{\alpha^2L_{P1}^2-1}\left[e^{\frac{-\alpha}{x_j-a_1}}-\frac{e^{\alpha}W}{cosh\left(\frac{x_j-a_1-W}{L_{P1}}\right)}+\frac{e^{-\alpha\left(x_j-a_1\right)}\cdot sinh\left(\frac{x_j-a_1-W}{L_{P1}}\right)}{L_{P1}cosh\left(\frac{x_j-a_1-W}{L_{P1}}\right)}\right] \quad (22)$$

where L_{P1} is the diffusion length of holes in the n layer. Due to the high electric field in the depletion region, all carriers generated will contribute to the total photo-current.

The current density in this region due to these carriers is given by:

$$J_{P2}=qF\left[e^{\frac{-\alpha}{x_j-a_1}}-e^{\frac{-\alpha}{x_j+a_2}}\right] \quad (23)$$

The differential equation for minority carriers in the p type region is given by:

$$D_n\frac{d^2_{nP}}{dx^2}-\frac{n_P-n_P\left(0\right)}{\tau_n}+\alpha Fe^{-\alpha x}=0 \quad (24)$$

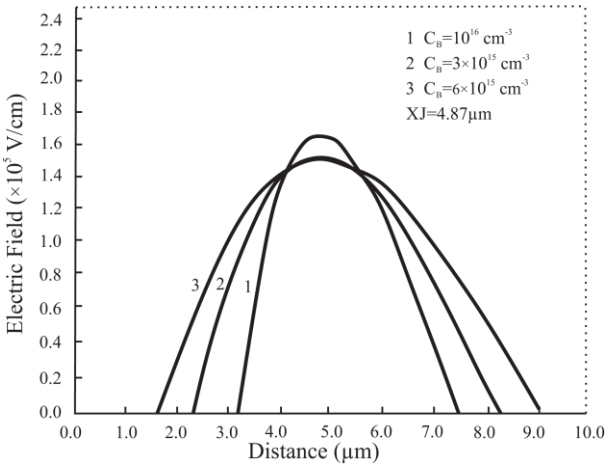

Fig. 5 Calculated electric field profile for n^+-n-p germanium avalanche photodiode for different bulk concentrations at a multiplication factor of 10.

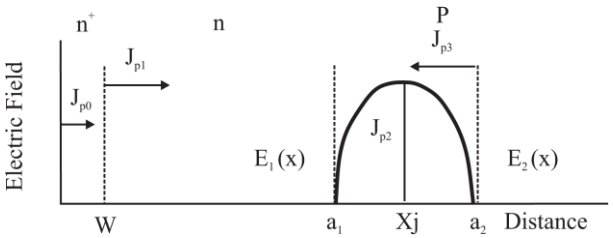

Fig. 6 Current density in each layer.

where D_n is the diffusion constant of electrons, n_P is the electron density, $n_P(0)$ is the equilibrium electron density, and τ_n is the life time of electrons.

3. For high reverse bias voltage

$$n_P=0, \text{ at } x=x_j-a_1 \quad (25)$$

$$n_P=n_{p0}, \text{ at } x\to\infty \quad (26)$$

4. The resulting electron photo-current density is then given by:

$$J_{P3}=\frac{qF\alpha L_n}{1+\alpha L_n}exp\left[-\alpha\left(x_j+a_2\right)\right] \quad (27)$$

where L_n is the diffusion length of electrons. The quantum efficiency is given by:

$$\eta=\frac{J_{P1}+J_{P2}+J_{P3}}{qF}=\frac{J_T}{qF} \quad (28)$$

The quantum efficiency of Germanium APD is strongly affected by the surface recombination velocity as shown in Fig. 7. This indicates that surface recombination velocity lowers the quantum efficiency in the wave length region shorter than 1.5 μm. So increasing the thickness of the n^+ layer is not desirable since it causes a reduction of quantum efficiency. The quantum efficiency can be improved by increasing the diffusion length of holes in the n^- layer by making $L_P > W$. Fig. 8 shows the Q.E. as a function of the wavelength λ for different values of junction depth x_j. It

is clear that the Q.E. decreases with increasing x_j. The Q.E. decreases as the bulk concentration increases as shown in Fig. 9, because the depletion region becomes wider and the photo-current inside the depletion region, which is the most important photo-current, increases.

3 Results Discussion and Comparison

In this section we will review the main findings of previous research and compare them with the results of this work.

Dion McIntosh and his group studied the Quantum Efficiency of the Gallium Phosphide (GaP) reach-through avalanche photodiodes (APDs). The APDs exhibited dark current less than a pico-ampere at unity gain. A quantum efficiency of 70% was achieved with a recessed window structure; this is almost two times higher than previous work [10].

Anand Singh and Rituparna Pal presented the design, fabrication and characteristics of HgCdTe Mid-Wave InfraRed avalanche photodiode (MWIR APD). The gain of 800 at -8 V bias voltage is measured in n^+-v-p^+ detector array with pitch size of 30 urn. The gain independent bandwidth of 6 MHz is achieved in the fabricated device. This paper also covers the status of HgCdTe and III-V material based IR-APD technology. These APDs having high internal gain and bandwidth are suitable for the detection of attenuated optical signals such as in the battle field conditions/long range imaging in defense and space applications. It provides a combined solution for both detection and amplification if the detector receives a very weak optical signal. HgCdTe based APDs provide high avalanche gain with low excess noise, high quantum efficiency, low dark current and fast response time [11].

Jeff Beck and his team studied an HgCdTe electron avalanche photodiode (e-APD) detector for lidar receivers, one application of which is integrated path differential absorption lidar measurements of such atmospheric trace gases as CO2 and CH4. The HgCdTe APD has a wide, visible to mid-wave-infrared, spectral response, high dynamic range, substantially improved sensitivity, and an expected improvement in operational lifetime. A demonstration sensor-chip assembly consisting of a 4.3 μm cutoff HgCdTe 4×4 APD detector array with 80 μm pitch pixels and a custom complementary metal–oxide–semiconductor readout integrated circuit was developed. The 4×4 detector system was characterized at 77 K with a 1.55 μm wavelength, 1 μs wide, laser pulse. The measured unit gain detector photon conversion efficiency was 91.1%. At 11 V bias the mean measured APD gain at 77 K was 307.8 with σ/mean uniformity of 1.23%. A gain-independent quantum-limited SNR of 80% of full theoretical was indicative of a gain-independent excess noise factor very close to 1.0 and the expected APD mode quantum efficiency [12].

Xiaoli Sun and his team presented in 2018 a linear mode photon counting HgCdTe avalanche photodiode (APD) focal plane array (FPA) detector for space lidar applications. An integrated detector cooler assembly (IDCA) was manufactured using a miniature Sterling cooler. The HgCdTe APD demonstrated a greater than 60% photon detection efficiency from 0.9 to 4.3 μm wavelength and a dark count rate less than 250,000/s. The IDCA cooled the FPA to 110 K from ambient room temperature at a total electrical power of 7 W [13].

Y. Kang, *et al*. published a paper about "Dark count probability and quantum efficiency of avalanche

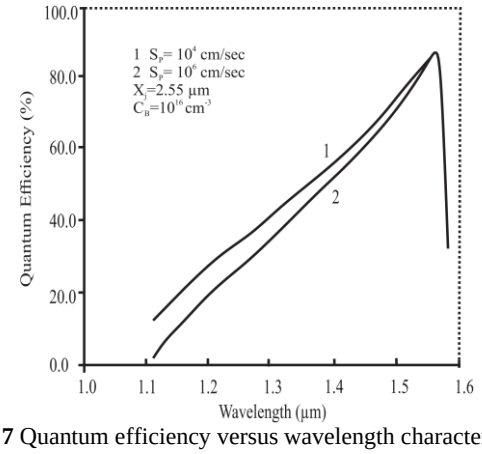

Fig. 7 Quantum efficiency versus wavelength characteristics as a parameter of surface recombination velocities.

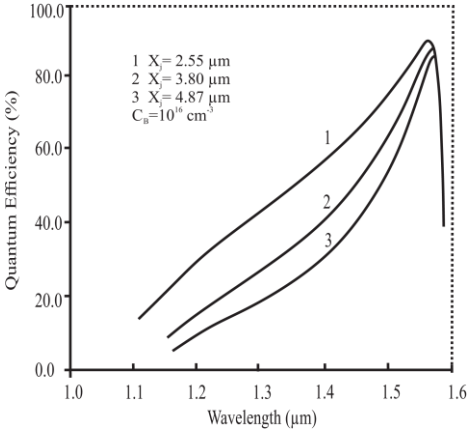

Fig. 8 Quantum efficiency versus wavelength characteristics as a parameter of junction depths.

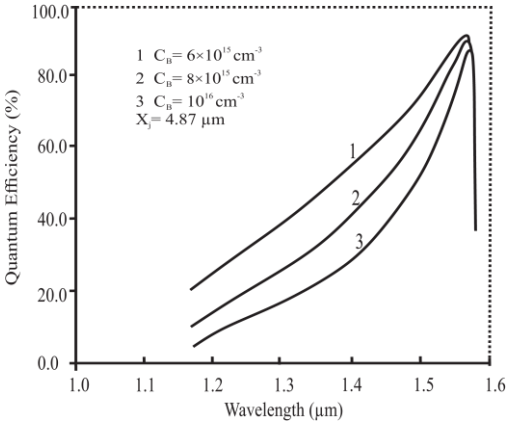

Fig. 9 Quantum efficiency versus wavelength characteristics as a parameter of bulk concentrations.

photodiodes for single-photon detection". They proposed a physical model that quantitatively describes the behavior of the dark count probability and single-photon quantum efficiency of avalanche diodes under conditions that allow these devices to be used for single-photon detection. The model shows analytically how various physical parameters such as dark current, dc gain, Geiger mode gain, carrier detrap time, pulse repetition rate, etc., can affect the dark count probability and single-photon quantum efficiency of a Geiger mode avalanche photodiode. Their theory agrees well with the experimental results [14].

4 Conclusion and Future Work

The Diode model has been successfully designed with a high quantum efficiency of 90% by adjusting the junction depth and the bulk concentration. In this design it is found that the optimum junction depth is 2.55 μm and the bulk concentration should be at 1×10^{16} cm^{-3} and the operating wavelength is 1550 nm. The breakdown voltage obtained from the output results is found to be 38.7 V, which is much smaller than that obtained for Silicon Avalanche photo-diode. As a future work multiplication noise, noise equivalent power (NEP) and the response time will be studied.

Acknowledgement

This work has been done at the Applied Science Private University, Amman, JORDAN, Faculty of Engineering, department of Electrical Engineering. The authors would like to thank this university for their strong support to this work.

References

[1] S. Olyaee, M. Izadpanah, and A. Najibi, "Analysis and modeling of avalanche photodiode using transfer matrix method," in *IEEE 8th International Symposium on Communication Systems, Networks & Digital Signal Processing (CSNDSP)*, pp. 1–5, 2012.

[2] D. Ong, K. Li, G. Rees, J. David, and P. Robson, "A simple model to determine multiplication and noise in avalanche photodiodes," *Journal of Applied Physics*, Vol. 83, No. 6, pp. 3426–3428, 1998.

[3] W. Kindt and H. Van Zeijl, "Modelling and fabrication of geiger mode avalanche photodiodes," *IEEE Transactions on Nuclear Science*, Vol. 45, No. 3, pp. 715–719, 1998.

[4] A. Bandyopadhyay, M. J. Deen, L. Tarof, and W. Clark, "A simplified approach to time-domain modeling of avalanche photodiodes," *IEEE Journal of Quantum Electronics*, Vol. 34, No. 4, pp. 691–699, 1998.

[5] R. Burden and J. Faires, "Numerical analysis 10/e IE," *Brooks/Cole Cengage Learning*, 2016.

[6] D. Prasad, *Introduction to numerical analysis, 3rd ed.* Narosa Publishing House, 2008.

[7] Y. Kang, H. Lu, Y. H. Lo, D. Bethune, and W. Risk, "Dark count probability and quantum efficiency of avalanche photodiodes for single-photon detection," *Applied Physics Letters*, Vol. 83, No. 14, pp. 2955–2957, 2003.

[8] F. Gity, J. Hayes, B. Corbett, and A. Morrison, "Modeling Ge/Si avalanche photodiodes," in *IEEE European Conference on Integrated Optics*, Apr. 2010.

[9] T. P. Lee and S. Chandrasekhar, "High-speed photonic devices," *Modern Semiconductors Device Physics (ed. SM Sze)*, pp. 409–472, 1998.

[10] D. McIntosh, Q. Zhou, Y. Chen, and J. C. Campbell, "High quantum efficiency gap avalanche photodiodes," *Optics Express*, Vol. 19, No. 20, pp. 19607–19612, 2011.

[11] A. Singh and R. Pal, "Infrared avalanche photodiode detectors," *Defence Science Journal*, Vol. 67, No. 2, pp. 159–168, 2017.

[12] J. Beck, T. Welch, and J. Abshire, "A highly sensitive multi-element HgCdTe e-APD detector for IPDA lidar applications," *Journal of Electronic Materials*, Vol. 43, No. 8, pp. 2970–2977, 2014.

[13] J. A. Xiaoli Sun and B. Hirasuna, "Single photon HgCdTe avalanche photodiode and integrated detector cooler assemblies for space lidar applications," in *Proceedings of SPIE 10659, Advanced Photon Counting Techniques XII, 106590C*, Orlando, Florida, United States, May 2018.

[14] Y. Kang, H. X. Lu, Y. H. Lo, D. S. Bethune, and W. Risk, "Dark count probability and quantum efficiency of avalanche photodiodes for single-photon detection," *Applied Physics Letters*, Vol. 83, No. 14, pp. 2955–2957, 2003.

T. Baldawi is an Associate Professor of Electronic Engineering. He got his B.Sc. degree in Electrical Engineering/Communications and Electronics from the University of Technology, Iraq, and his M.Sc. and Ph.D. degrees in Electronics from Montpellier University of Science and Technology, France in 1982. He worked for 19 years as Associate Professor of Electronics at the Applied Science Private University ASU, Jordan. His research interest are electronic circuit design, noise in electronic devices and photo-detectors.

A. Abuelhaija is an Assistant Professor in the Department of Electrical Engineering at Applied Science Private University, Amman, Jordan, where he received his B.Sc. in Communications and Electronics Engineering in 2007. He received his Master degree and Ph.D. in Electrical Engineering from Duisburg-Essen University in 2010 and 2016, respectively. His research interests are in the area of antennas and RF technology. From 2012 to 2014, he works as Research Assistant at Erwin L. Hahn Institute for Magnetic Resonance Imaging, Essen, and from 2014 to 2016 as Research Assistant at the Department of Microwave and RF Technology at Duisburg-Essen University.